

# High Contrast X-ray Speckle from Atomic-Scale Order in Liquids and Glasses

S. O. Hruszkewycz,<sup>1</sup> M. Sutton,<sup>2</sup> P. H. Fuoss,<sup>1</sup> B. Adams,<sup>3</sup> S. Rosenkranz,<sup>1</sup> K. F. Ludwig Jr.,<sup>4</sup> W. Roseker,<sup>5</sup> D. Fritz,<sup>6</sup> M. Cammarata,<sup>6</sup> D. Zhu,<sup>6</sup> S. Lee,<sup>5,6,\*</sup> H. Lemke,<sup>6</sup> C. Gutt,<sup>5</sup> A. Robert,<sup>6</sup> G. Grübel,<sup>5</sup> and G. B. Stephenson<sup>1,7</sup>

<sup>1</sup>Materials Science Division, Argonne National Laboratory, Argonne, Illinois 60439 USA

<sup>2</sup>Department of Physics, McGill University, Montreal, H3A2T8 Canada

<sup>3</sup>X-ray Science Division, Argonne National Laboratory, Argonne, Illinois 60439 USA

<sup>4</sup>Department of Physics, Boston University, Boston, Massachusetts, 02215 USA

<sup>5</sup>HASYLAB, Deutsches Elektronen-Synchrotron, Hamburg, Germany

<sup>6</sup>Linac Coherent Light Source, SLAC National Accelerator Laboratory, Menlo Park, California 94025 USA

<sup>7</sup>Advanced Photon Source, Argonne National Laboratory, Argonne, Illinois 60439 USA

(Dated: October 31, 2018)

The availability of ultrafast pulses of coherent hard x-rays from the Linac Coherent Light Source opens new opportunities for studies of atomic-scale dynamics in amorphous materials. Here we show that single ultrafast coherent x-ray pulses can be used to observe the speckle contrast in the high-angle diffraction from liquid Ga and glassy Ni<sub>2</sub>Pd<sub>2</sub>P and B<sub>2</sub>O<sub>3</sub>. We determine the thresholds above which the x-ray pulses disturb the atomic arrangements. Furthermore, high contrast speckle is observed in scattering patterns from the glasses integrated over many pulses, demonstrating that the source and optics are sufficiently stable for x-ray photon correlation spectroscopy studies of dynamics over a wide range of time scales.

PACS numbers: 41.60.Cr, 61.20.-p, 61.43.Dg, 51.50.th

Ever since the initial observation of speckle in the diffraction of coherent short-wavelength x-rays [1], it has been recognized that coherent x-ray techniques have the potential to provide powerful new probes of *atomic scale* structure and dynamics in non-crystalline systems, analogous to the techniques developed to study disorder at much larger length scales using coherent visible light [2]. In particular, x-ray photon correlation spectroscopy (XPCS) has been developed using high-brightness synchrotron x-ray sources to observe equilibrium and non-equilibrium dynamics in diverse systems [3, 4]. A limiting factor in the development of XPCS for atomic scale studies has been the signal level that can be obtained. Almost all XPCS studies to date probe relatively large length scale ( $> 10$  nm) structures, for example via small-angle scattering from colloids and polymers [5–9] or diffuse scattering near Bragg peaks of crystals [10–12], because of their larger scattering cross sections compared with atomic-scale fluctuations, and the limited coherent x-ray power available. The first XPCS observation of truly atomic-scale dynamics was obtained only recently [13] in a study of diffusion in Cu-Au on relatively slow timescales ( $> 10$  s).

One of the scientific drivers for the new generation of intense, coherent hard x-ray free electron laser sources, such as the Linac Coherent Light Source (LCLS) at SLAC National Accelerator Laboratory, has been their potential for XPCS studies to open a new frontier at the natural time scales of even the fastest condensed matter systems, e.g. atomic diffusion in liquids [14, 15]. The combination of femtosecond pulses and atomic resolution speckle provides unprecedented opportunities to test theories of liquid structure and dynamics, such as the intriguing predictions that have recently emerged regarding the complex dynamics of both diffusive [16] and vibrational [17] modes in liquids and glasses. Ultrafast XPCS provides a time-domain probe complementary

to inelastic scattering, capable of studies of sub-micron volumes and non-equilibrium dynamics. To reach femtosecond time scales, which are much faster than the time resolution of imaging detectors, a pulse split-and-delay technique has been proposed [14, 15, 18–20] in which the correlation time is determined from the change in contrast of the sum of two speckle patterns, as a function of the delay time between the patterns. Although LCLS provides a huge leap in available coherent flux and accessible time scales, the high number of photons delivered in a single pulse poses challenges in avoiding x-ray effects on the sample during a dynamics measurement [14, 15]. A primary issue is whether accurate contrast values can be extracted from the relatively weak speckle patterns expected in optimized XPCS studies. Likewise, the variations in pulse energy and position pose potential challenges for speckle measurements. Here, we report the first observation of high contrast x-ray speckle from the atomic scale structure in both liquid and glass samples. These were obtained using femtosecond hard x-ray pulses from the LCLS. We present an effective analysis procedure to extract contrast, show the dependence of contrast on experimental conditions, report the observed perturbation thresholds of various samples, and discuss the design of an optimized atomic resolution XPCS experiment.

We recorded speckle patterns from three samples: Ga heated into the liquid phase at 35 C, and two glasses at room temperature, Ni<sub>2</sub>Pd<sub>2</sub>P and B<sub>2</sub>O<sub>3</sub>. The average structure factors of these systems have all been previously characterized using standard scattering methods [21–23]. Experiments were carried out with the XPP instrument at LCLS, using a Si (111) monochromator with  $1.4 \times 10^{-4}$  bandwidth set to 7.99 keV photon energy, and a 70 fs electron pulse width [24]. The average unattenuated x-ray pulse energy was typically  $\sim 1 \times 10^{10}$  and  $\sim 4 \times 10^{10}$  photons per pulse for single-pulse or multi-

pulse images, respectively [24], although there was a very broad distribution of pulse energies with a maximum typically 5 times the mean. The scattering geometries were chosen to provide coherent illumination conditions that would fulfill the requirements to produce high-contrast speckle patterns [25, 26] and to resolve this pattern at the detector. Measurements were made with a beam focused to  $1.7 \mu\text{m}$  FWHM at the sample using Be compound refractive lenses. Diffraction patterns were recorded using a direct-x-ray-detection CCD with  $20 \mu\text{m}$  square pixels at a distance from the sample of  $L = 18$  to  $142$  cm, positioned at an average scattering angle corresponding to the peak in the strongest amorphous scattering ring. For Ga and  $\text{Ni}_2\text{Pd}_2\text{P}$ , we employed bulk samples in reflection geometry at  $Q \approx 2.60$  and  $2.95 \text{ \AA}^{-1}$ , respectively; for  $\text{B}_2\text{O}_3$ , we employed a fiber of  $18 \mu\text{m}$  thickness in transmission geometry at  $Q \approx 1.62 \text{ \AA}^{-1}$ . Unattenuated single-pulse speckle patterns were recorded from all samples. To investigate the stability of the experimental setup and perturbation of the sample by the x-ray beam, we also recorded speckle patterns from the glass samples that were sums of multiple attenuated pulses.

Figure 1(a) shows a typical region of amorphous scattering viewed by the detector at  $L = 37$  cm for liquid Ga. This image of the average scattering was obtained by summing many single-pulse patterns and binning the pixels to smooth out the photon statistics. Figure 1(c) gives a small region of one of the single-pulse patterns, showing the individual photon hits. Since the width of the x-ray pulses is expected to be shorter than the time scale of equilibrium diffusive and vibrational motions of the atoms in the liquid, such single-pulse diffraction patterns should exhibit high speckle contrast if the x-ray optics are sufficiently free of aberrations, the detector resolution and noise characteristics are adequate, and the x-ray pulse does not disturb the atomic positions in the sample on the time scale of the measurement. A critical issue is to understand the accuracy with which the contrast can be determined from such weak speckle patterns.

Recent studies have obtained the contrast in speckle patterns from the normalized variance of the signal distribution on the detector [27, 28]. When the photon density is low, the variance contains a large contribution from the counting statistics of individual photons in addition to the contrast [3, 18, 24]. Our approach to extracting the contrast is to compare the observed probability for  $k$  photons arriving in a single detector pixel to the negative binomial distribution expected for a speckle pattern of a given contrast [29]

$$P(k) = \frac{\Gamma(k+M)}{\Gamma(M)\Gamma(k+1)} \left(1 + \frac{M}{\bar{k}}\right)^{-k} \left(1 + \frac{\bar{k}}{M}\right)^{-M}, \quad (1)$$

where  $\bar{k}$  is the mean photon density (counts per pixel),  $M$  is the number of modes in the speckle pattern, and  $\Gamma$  is the gamma function. The speckle contrast factor  $\beta \equiv M^{-1}$  has a maximum value of unity for a single-mode distribution, and it drops to zero as  $M$  increases. For  $M \rightarrow \infty$ , Eq. (1) approaches the familiar Poisson distribution for uncorrelated

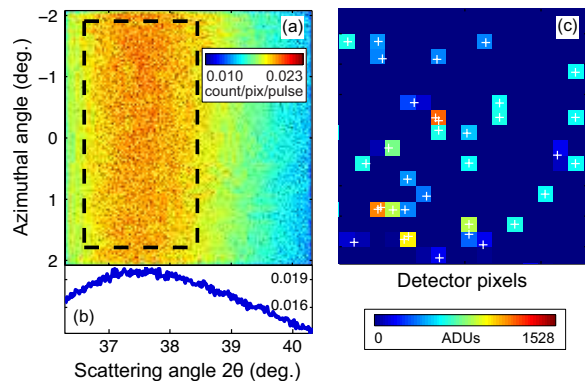


FIG. 1: (Color online) (a) Average scattering of liquid Ga integrated over 309 pulses from LCLS. Detector at  $L = 37$  cm from sample subtends scattering angles including the main amorphous scattering ring at  $Q = 2.60 \text{ \AA}^{-1}$ . Dashed box shows region of pixels used in contrast analysis. (b) Average photon density vs. scattering angle. (c) Expansion of small region of a single-pulse scattering pattern showing signal in analog-to-digital units (ADUs) from individual photons, and assignment of photon positions.

photon positions,  $P(k) = \bar{k}^k \exp(-\bar{k})/k!$ . The contrast factor will be less than unity if the conditions are not met for the required transverse or longitudinal coherence of the incident beam [25, 26], if the detector pixels are too large to fully resolve the speckle, or if the sample is not static on the time scale over which the pattern is recorded. It is this latter effect that allows the sample dynamics to be extracted from measurements of speckle contrast. In particular, if we record the sum of two speckle patterns of contrast factor  $\beta_0$  from two equal-energy x-ray pulses separated by a time  $\tau$ , the contrast factor of the sum will drop from  $\beta_0$  to  $\beta_0/2$  as  $\tau$  is varied from much less than to much more than the correlation time of the sample dynamics [15, 29].

To accurately extract the contrast in these weak speckle patterns, we first employ a “droplet algorithm” [24, 30] to locate the positions of each detected photon by fitting each recorded pattern. Typical results for extracted photon positions are shown in Fig. 1(c). Experimental probabilities  $P(k)$  are obtained by choosing a region of pixels that has nearly uniform  $\bar{k}$  and  $Q$ , i.e. along the peak of the amorphous scattering ring as shown in Fig. 1(a), binning the photon positions into the detector pixels, and determining the fraction of pixels that have  $k$  photons. Figure 2 shows the experimental probabilities for  $k = 1$  to  $4$  for 309 speckle patterns having various mean count densities  $\bar{k}$ . We obtained a contrast factor  $\beta$  for each speckle pattern by analyzing the  $P(k)$  as described in the supplemental material [24]. The weighted average of these values gives  $\langle\beta\rangle = 0.276 \pm 0.004$  for liquid Ga and  $L = 37$  cm. While the speckle patterns with highest  $\bar{k}$  provide the highest accuracy contrast values, the full distribution of weaker and stronger speckle patterns obtained (due to the wide incident pulse energy variation characteristic of monochromatic hard x-ray experiments at LCLS) verifies the predicted  $\bar{k}$  dependences given by the negative binomial distribution. These measurements on liquid Ga represent the first observation of

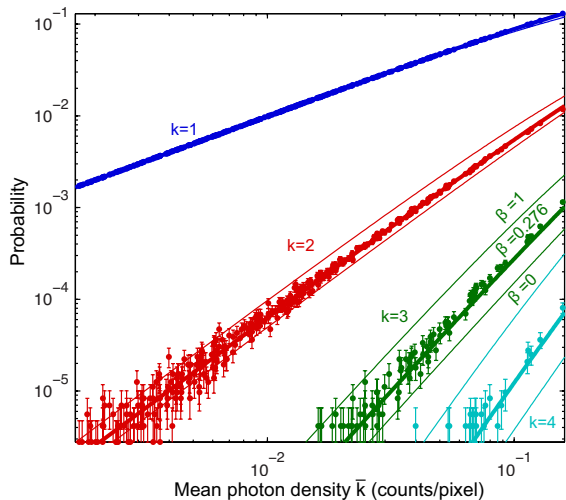


FIG. 2: (Color online) Observed probability of  $k = 1$  to 4 photons within a pixel as a function of mean photon density  $\bar{k}$ , for 309 single-pulse speckle patterns from liquid Ga for  $L = 37$  cm. Thick curve is negative binomial distribution with  $\beta = 0.276$ ; thin curves show limiting distributions for  $\beta = 1$  and  $\beta = 0$ .

TABLE I: Experimental parameters, extracted average contrast factors  $\langle\beta\rangle$ , and calculated maximum contrast factor  $\beta_{calc}$  for speckle patterns from Ga liquid,  $\text{Ni}_2\text{Pd}_2\text{P}$  glass, and  $\text{B}_2\text{O}_3$  glass. The parameter  $L$  is the sample-to-detector distance, “pulses” is the number of consecutive LCLS pulses integrated in each speckle pattern,  $n_{patt}$  gives the number of speckle patterns included in the contrast analysis,  $\langle I_0 \rangle$  gives the average number of photons per pulse incident on the sample (after any attenuation), and  $\langle \bar{k} \rangle$  is the average of the mean photon densities in this set of patterns. The number of pixels used was  $n_{pix} = 3.6, 7.2, \text{ or } 13.2 \times 10^5$  for  $L = 18, 35$  to 37, or 142 cm, respectively.

$L$ (cm)	pulses	$n_{patt}$	$\langle I_0 \rangle$ (ct/pulse)	$\langle \bar{k} \rangle$ (ct/pix)	avg. contrast factor $\langle\beta\rangle$	$\beta_{calc}$
<b>Ga</b>						
37	1	309	$1.1 \times 10^{10}$	0.019	$0.276 \pm 0.004$	0.307
<b><math>\text{Ni}_2\text{Pd}_2\text{P}</math></b>						
18	1	29	$1.5 \times 10^{10}$	0.072	$0.245 \pm 0.006$	0.349
18	500	60	$1.7 \times 10^7$	0.065	$0.276 \pm 0.005$	0.349
18	500	47	$8.4 \times 10^7$	0.184	$0.156 \pm 0.002$	0.349
35	1	81	$1.2 \times 10^{10}$	0.016	$0.360 \pm 0.010$	0.645
35	500	40	$1.8 \times 10^7$	0.014	$0.492 \pm 0.022$	0.645
35	500	60	$8.7 \times 10^7$	0.041	$0.319 \pm 0.006$	0.645
142	500	20	$4.4 \times 10^8$	0.016	$0.408 \pm 0.019$	0.713
<b><math>\text{B}_2\text{O}_3</math></b>						
37	10	9	$8.6 \times 10^9$	0.007	$0.291 \pm 0.057$	0.446
37	100	20	$1.9 \times 10^{10}$	0.056	$0.195 \pm 0.005$	0.446
37	500	61	$3.6 \times 10^8$	0.017	$0.356 \pm 0.014$	0.446

speckle from the atomic-scale order in a liquid.

To investigate whether the stability of the source and experiment will affect the contrast in multi-pulse XPCS experiments, and to understand the thresholds for irreversible perturbation of the sample structure by the incident x-ray pulses, we studied two glasses where the liquid-like atomic arrange-

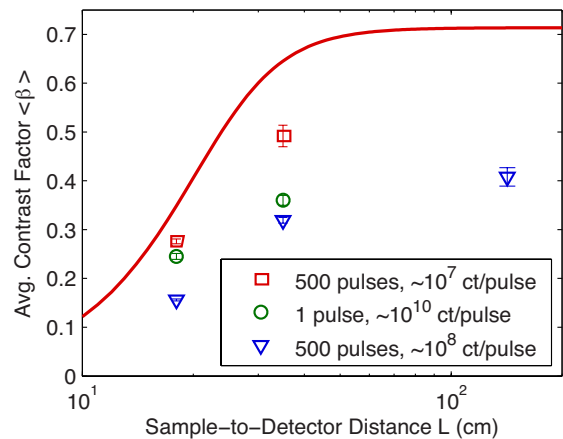


FIG. 3: (Color online) Contrast factor  $\langle\beta\rangle$  vs. sample-to-detector distance  $L$  for the  $\text{Ni}_2\text{Pd}_2\text{P}$  glass. Curve is calculation for a static sample; symbols are observed values for single-pulse and 500-pulse images with different  $\langle I_0 \rangle$  values shown in legend.

ment should be static. For the metallic glass  $\text{Ni}_2\text{Pd}_2\text{P}$ , we collected not only single-pulse speckle patterns without attenuation of the incident beam (like we did with liquid Ga), but also sums of 500 consecutive attenuated pulses. The values of  $\langle\beta\rangle$  extracted for both single-pulse and attenuated 500-pulse speckle patterns at three different values of sample-to-detector distance  $L$  are given in Table I. Scattering from the low-atomic-number glass  $\text{B}_2\text{O}_3$  was too weak to obtain values of  $\langle\beta\rangle$  from single pulses under the available experimental conditions; Table I gives results for multiple-pulse patterns with various  $\langle I_0 \rangle$ .

The observed  $\langle\beta\rangle$  values can be compared with those calculated for a static sample using an incident beam with full transverse coherence but non-zero photon energy bandwidth, and a detector with non-zero pixel size. These resolution effects reduce the calculated static contrast factor  $\beta_{calc}$  from unity depending upon the size of the illuminated volume, the scattering angle, and the sample-to-detector distance  $L$  [24]. Table I gives  $\beta_{calc}$  values for each of the samples and experimental conditions. The observed  $\langle\beta\rangle$  value for liquid Ga is 90% of the corresponding  $\beta_{calc}$ , indicating that the ultrafast x-ray pulses have effectively frozen the motion of the atoms, giving a coherent diffraction snapshot of their arrangement in the liquid. It also indicates that the unattenuated, focused x-ray beam does not significantly alter the atomic arrangements in liquid Ga during the time of the pulse, even though the energy deposited in the illuminated sample volume ( $\sim 30$  eV per atom per average pulse) is typically enough to vaporize it on a longer time scale [24].

Figure 3 shows the measured contrast factor values for the  $\text{Ni}_2\text{Pd}_2\text{P}$  glass compared with  $\beta_{calc}$  as a function of  $L$ . The overall dependence of the observed  $\langle\beta\rangle$  on  $L$  agrees with that of the calculation. The highly attenuated 500-pulse patterns have contrast factors that are 75-80% of  $\beta_{calc}$ , indicating not only that there is minimal disturbance of the sample by the x-ray pulses, but that the contrast is not greatly lowered by vari-

ations in the pulse energy and position of the incident beam or other instabilities of the experimental setup. The measured  $\langle\beta\rangle$  values are somewhat smaller for 500-pulse patterns with less attenuation or single pulse patterns with no attenuation, consistent with some disturbance of the sample structure by the incident beam. For the single-pulse data, the energy density deposited is higher for Ni<sub>2</sub>Pd<sub>2</sub>P ( $\sim 75$  eV or  $\sim 95$  eV per atom per average pulse) than for Ga owing to its shorter absorption length, which agrees with the observed higher disturbance during single pulses [24]. Based on the maximum incident pulse energies in the attenuated 500-pulse sequences, the threshold for longer time (inter-pulse) sample disturbance effects occurs at about 1 eV per illuminated atom absorbed energy. The dataset for B<sub>2</sub>O<sub>3</sub> indicates that this threshold is also about 1 eV per atom in this “light” material, corresponding to a higher incident fluence because of its longer absorption length. Based on the observed melting threshold for Ni<sub>2</sub>Pd<sub>2</sub>P, we estimate that the deposited pulse energy is thermalized in a volume 50 times larger than the illuminated volume, consistent with the expected spread of the electron/photon/phonon cascade generated by x-ray absorption [24], resulting in a maximum temperature rise of  $0.02 \text{ eV}/3k_B \approx 80 \text{ K}$ .

These measurements allow an analysis of the feasibility of femtosecond XPCS experiments using the split-pulse technique [14, 15, 18]. The figure of merit for such measurements is the signal-to-noise ratio for  $\beta$ , which for low  $k$  is determined by fluctuations in the small number of  $k = 2$  events and can be expressed as [24]  $\beta/\sigma_\beta = \beta k [n_{pix} n_{patt} / 2(1 + \beta)]^{1/2}$ . This expression agrees well with the observed accuracy of  $\langle\beta\rangle$  given in Table I, indicating that other potential experimental contributions to the uncertainty are negligible. If we use a detector capable of recording  $n_{pix} = 10^6$  pixels at the full LCLS repetition rate of 120 Hz, to give  $n_{patt} = 4 \times 10^4$  in six minutes per delay time, and extrapolate the measured relationships between  $k$  and  $I_0$  [24], the pulse energies needed to give a signal-to-noise ratio of 5 sufficient for XPCS are  $I_0 = 6, 0.3,$  or  $0.13 \times 10^8$  photons per pulse, corresponding to sample temperature rises of 3 to 7 K, for B<sub>2</sub>O<sub>3</sub>, Ga, or Ni<sub>2</sub>Pd<sub>2</sub>P, respectively. These temperature rises are significantly below the 80 K threshold for structural disturbance by diffusive atomic rearrangement that we observed for the glass samples, indicating that even more sensitive samples and processes can be studied.

The new analysis technique presented here allows the accurate determination of speckle contrast using the weak patterns obtained under conditions in which the x-ray pulses from a free electron laser do not disturb the sample dynamics. We observe high contrast factors in x-ray speckle patterns from liquids and glasses obtained with ultrafast pulses, demonstrating that XPCS can be used to observe their atomic-scale dynamics on times scales down to the femtosecond range. We find that the atomic motions associated with x-ray damage occur on time scales shorter than the x-ray pulse width used here for deposited energy densities greater than about 50 eV per illuminated atom [24]. This provides guidance for design of studies in which single-pulse speckle patterns are analyzed to

obtain atomic-scale structural information.

Special thanks go to T. Hufnagel for the use of his metallic glass laboratory and to A. Zholents for insightful comments. X-ray experiments were carried out at LCLS at SLAC National Accelerator Laboratory, an Office of Science User Facility operated for the U.S. Department of Energy (DOE) Office of Science by Stanford University. Work at Argonne National Laboratory supported by the DOE Office of Basic Energy Sciences under contract DE-AC02-06CH11357. Supporting electron microscopy was accomplished at the Electron Microscopy Center for Materials Research at Argonne, a DOE Office of Science User Facility. The work of KFL on this project was supported by the U.S. DOE Office of Science, Office of Basic Energy Sciences under DE-FG02-03ER46037.

- 
- \* Present address: Physical Metrology Division, Korea Research Institute of Standards and Science, Daejeon 305-340 S. Korea.
- [1] M. Sutton et al., *Nature* **352**, 608 (1991).
  - [2] B. J. Berne and R. Pecora, *Dynamic Light Scattering with Applications*, (Wiley, 1976).
  - [3] F. Livet, *Acta Cryst. A* **63**, 87 (2007).
  - [4] G. B. Stephenson, A. Robert, and G. Grübel, *Nature Mater.* **8**, 702 (2009).
  - [5] S. B. Dierker et al., *Phys. Rev. Lett.* **75**, 449 (1995).
  - [6] D. O. Riese et al., *Phys. Rev. Lett.* **85**, 5460 (2000).
  - [7] D. Pontoni et al., *Phys. Rev. Lett.* **90**, 188301 (2003).
  - [8] S. G. J. Mochrie et al., *Phys. Rev. Lett.* **78**, 1275 (1997)
  - [9] D. Lumma et al., *Phys. Rev. Lett.* **86**, 2042 (2001).
  - [10] S. Brauer et al., *Phys. Rev. Lett.* **75**, 449 (1995).
  - [11] O. G. Shpyrko et al., *Nature* **447**, 68 (2007).
  - [12] M. S. Pierce et al., *Phys. Rev. Lett.* **103**, 165501 (2009).
  - [13] M. Leitner, B. Sepiol, L.-M. Stadler, B. Pfau, and G. Vogl, *Nature Mater.* **8**, 717 (2009).
  - [14] G. B. Stephenson et al. in *LCLS: The First Experiments* (2000), [www-ssrl.slac.stanford.edu/lcls/papers/lcls\\_experiments\\_2.pdf](http://www-ssrl.slac.stanford.edu/lcls/papers/lcls_experiments_2.pdf).
  - [15] G. Grübel, G. B. Stephenson, C. Gutt, H. Sinn, and T. Tschentscher, *Nucl. Instrum. Meth. B* **262**, 357 (2007).
  - [16] J. S. Langer, *Phys. Rev. E* **78**, 051115 (2008).
  - [17] H. Shintani and H. Tanaka, *Nature Mater.* **7**, 870 (2008).
  - [18] C. Gutt et al., *Optics Express* **17**, 55 (2009).
  - [19] W. Roseker et al., *Optics Letters* **34**, 1768 (2009)
  - [20] W. Roseker et al., *J. Synchr. Rad.* **18**, 481 (2011)
  - [21] M.C. Bellissent-Funel, P. Chieux, D. Levesque, and J.J. Weis, *Phys. Rev. A.* **39**, 6310 (1989).
  - [22] T. Egami, W. Dmowski, Y. He, and R.B. Schwarz, *Metall. and Mater. Trans. A* **29**, 1805 (1998).
  - [23] R. L. Mozzi and B. E. Warren, *J. Appl. Cryst.* **3**, 251 (1970).
  - [24] See Supplemental material.
  - [25] P. N. Pusey, Statistical properties of scattered radiation, in *Photon Correlation Spectroscopy and Velocimetry*, ed. H. Z. Cummins and E. R. Pike (Plenum, New York, 1974).
  - [26] M. Sutton, Coherent x-ray diffraction, in *Third-Generation Hard X-ray Synchrotron Radiation Sources: Source Properties, Optics, and Experimental Techniques*, ed. D. M. Mills (Wiley, New York, 2002).
  - [27] C. Gutt et al., *Phys. Rev. Lett.* **108**, 024801 (2012).
  - [28] K. Ludwig, *J. Synchr. Rad.* **19**, 66 (2012).
  - [29] J. W. Goodman, *Speckle Phenomena in Optics : Theory and*

*Applications* (Roberts & Co., Englewood, Colo., 2007).  
[30] F. Livet et al., Nucl. Instrum. Meth. A **451**, 596 (2000).